ISSN 1028-3358, Doklady Physics, 2017, Vol. 62, No. 5, pp. 248–252. © Pleiades Publishing, Ltd., 2017.
Original Russian Text © P.A. Perezhogin, V.P. Dymnikov, 2017, published in Doklady Akademii Nauk, 2017, Vol. 474, No. 1, pp. 36–40.

MECHANICS

Modeling of Quasi-Equilibrium States of a Two-Dimensional Ideal Fluid

P. A. Perezhogin[a,b]* and Academician V. P. Dymnikov[a]

Received October 19, 2016

Abstract—Contrary to a viscous fluid at high Reynolds numbers, the equations of a two-dimensional ideal fluid have an infinite number of invariants, the presence of which complicates both its statistical description and the numerical modeling. In this study, the numerical modeling of quasi-equilibrium states of an ideal fluid is carried out at a high resolution of 8192^2 within the framework of two models: the Arakawa approximations with two quadratic invariants and the approximations of the equations for a viscous fluid in the asymptotic case of low viscosity. The possibility of application of the theory of Cesaro convergence (time averaging) for the solution of the problem of unsteadiness of final states and the problem of achievement of equilibrium states are considered.

DOI: 10.1134/S1028335817050032

The equations of a two-dimensional ideal fluid have the form

$$\frac{\partial \omega}{\partial t} + J(\psi, \omega) = 0, \quad \Delta\psi = \omega, \tag{1}$$

where ψ is the stream function, ω is the vorticity, and $J(\psi, \omega) = -\frac{\partial \psi}{\partial y}\frac{\partial \omega}{\partial x} + \frac{\partial \psi}{\partial x}\frac{\partial \omega}{\partial y}$ is the Jacobian. We consider these equations on a periodic square $\Omega = [0, 2\pi)^2$. The equations have laws of conservation of energy

$$E = -\frac{1}{2}\int_\Omega \psi\omega dx$$

and an infinite number of casimirs

$$C_n = \int_\Omega \omega^n dx,$$

among which an important role is played by enstrophy

$$Z = \frac{1}{2}\int_\Omega \omega^2 dx.$$

The invariancy of all casimirs is equivalent to the preservation of distribution of vorticity over the areas $dS/S = \gamma(\omega)d\omega$, where dS is an element of the area on which the vorticity belongs to the interval $(\omega, \omega + d\omega)$.

The equations of the viscous fluid are obtained by adding the dissipation term (in this study, we deal with the biharmonic viscosity) on the right-hand side:

$$\frac{\partial \omega}{\partial t} + J(\psi, \omega) = -\nu\Delta^2\omega, \quad \Delta\psi = \omega. \tag{2}$$

The finite-dimensional ideal fluid is obtained after applying discretization having the laws of conservation of quadratic invariants to Eqs. (1) of an ideal fluid.

In all three systems, large-scale flows having a similar structure are formed and, in fine scales, serious differences are observed. The possibility of obtaining quasi-equilibrium states can be explained with the help of the theory of Kraichnan cascades [8], according to which the enstrophy passes into fine scales and the energy goes into large scales. In the case of a viscous fluid, the enstrophy is dissipated in fine scales, and the dissipation of energy tends to zero on the time scales of formation of the large-scale flows in the case of asymptotically fine viscosity $\nu \to +0$. Such a scenario is called selective decay [10], and, as a result, the energy accumulates on the largest Fourier harmonics forming large-scale coherent structures. The coherent structures also are formed in an ideal fluid and in its finite-dimensional approximations; however, contrary to the viscous case, the enstrophy is accumulated in the finest scale of the system and it results in the formation of fine-scale fluctuations, which have no finite scale in the case of an ideal fluid and are determined by the scale of the computing grid in the case of finite-dimensional approximations.

Large-scale coherent structures are close to the steady solution and, for this reason, have the approximate dependence $\omega = F(\psi)$. This dependence can be

[a] *Institute of Numerical Mathematics, Russian Academy of Sciences, Moscow, 119333 Russia*
[b] *Moscow Institute of Physics and Technology, (State University) Dolgoprudnyi, Moscow oblast, 141700 Russia*
**e-mail: pperezhogin@gmail.com*

found with the help of the statistical theory for the equations of an ideal fluid and its finite-dimensional approximations because both systems are Hamiltonian. In each case, it is possible to use the mean field theory [12] if only to agree to consider the finite-dimensional case in the limit of the infinite resolution [4]. The mean field theory predicts the occurrence of the equilibrium states described by the average field $\overline{\omega}$, which sets the spectrum of energy, and by the fluctuations around the average field, which determine the level of casimirs (hereinafter, the overline designates space averaging). The predictions of the theory for an ideal fluid and its finite-dimensional approximations differ: in the case of an ideal fluid, the arbitrary monotonic function $\overline{\omega} = F(\overline{\psi})$ is possible depending on the level of casimirs at the initial moment of time and, in the case of finite-dimensional approximations, the theory predicts the linear relation $\overline{\omega} = -\overline{\psi}$, which means the full condensation of energy on the largest Fourier harmonic [4]. We note that the states arising in the numerical experiments are not equilibrium and have the functional dependence $\overline{\omega} = F(\overline{\psi})$ only approximately. For this reason, we call them quasi-equilibrium or final.

In the case of free three-dimensional turbulence, the problem of the similarity of the large-scale flows arising in a viscous fluid and in finite-dimensional approximations of the ideal fluid is considered in detail in [5, 7]. Contrary to the two-dimensional case, in three-dimensional turbulence, the absence of a wide class of laws of conservation results in the triviality of equilibrium states (the viscous fluid fades to zero and, in the finite-dimensional approximations, the energy is distributed uniformly over the Fourier harmonics). Nevertheless, it was shown that the large-scale dynamics proves to be similar in the process of establishing equilibrium. In the two-dimensional case, no similar comparison of the two models has been carried out until now. We present here only the most modern works devoted to a viscous fluid [11, 6] and the finite-dimensional approximations [13]. We compare these two models and pay attention to structures of the solution recently found in the viscous fluid, such as the step shape of large vortices and the presence of fine vortices in quasi-equilibrium states [6].

Contrary to the predictions of the mean field theory, the final states prove to be unsteady: large vortices drift [11, 6]. For this reason, we consider the problem on the type of convergence of solutions of the equations of an ideal fluid to the equilibrium states. It is obvious that there can be no convergence of the type $\overline{\omega} = \lim_{t\to+\infty} \overline{\omega}(x,t)$ in the presence of large-scale unsteadiness. As an alternative, it is possible to consider the Cesaro convergence:

$$\langle\omega\rangle = \lim_{t\to+\infty}\langle\omega\rangle_0^t = \lim_{t\to+\infty}\frac{1}{t}\int_0^t \omega(\mathbf{x},t')dt'.$$

For ergodic systems, such a process converges to the equilibrium state, i.e., $\lim_{t\to+\infty}\langle\omega\rangle_0^t = \overline{\omega}$. As can be seen from this formula, time averaging is one more way of singling out the average field in addition to space averaging. Because an ideal fluid is not an ergodic system ($\overline{\omega} \neq \langle\omega\rangle$), we should investigate the coherent structures $\langle\omega\rangle = G(\langle\psi\rangle)$ and compare them to classical coherent structures $\overline{\omega} = F(\overline{\psi})$. If we reformulate the results of the mean field theory in terms of the Cesaro convergence, it is possible to solve two problems at once: the problem of achievement of equilibrium states and the problem of unsteadiness of final states. In this investigation, we used the Cesaro-convergence theory described in detail in [1].

The numerical experiments are carried out for the viscid and inviscid problems at the resolutions of 512^2, 2048^2, 8192^2. The values of biharmonic viscosity are

Resolution	512^2	2048^2	8192^2
ν	1.875×10^{-11}	7.3242×10^{-14}	2.86×10^{-16}

In both cases, the Arakawa approximation with two quadratic invariants [2] and the Crank-Nicolson scheme in time was chosen. The implicit scheme is solved by the fixed-point iteration with a relative accuracy of conservation of quadratic invariants 10^{-10} for the whole time of calculation. For comparison, the accuracy amounted to 10^{-4} in [13]. The initial vorticity field consists of 16×16 steps with constant values of

$$\omega_i \in \{-1+h, -1+3h, \ldots, 1-h\}, \text{ where } h = 1/256,$$

which are randomly distributed over steps (see Fig. 1), but each value is encountered only once, and the distribution is the same for all experiments. The time of calculation amounts to $T = 10\,000$ at the highest velocity $V_{\max} \approx 0.2$. If we determine the large eddy turnover time as $T_{\text{eddy}} = L/V_{\max}$, $T_{\text{eddy}} \approx 30$, then the time of calculation amounted to $T \approx 315T_{\text{eddy}}$. At low resolutions of 512^2, 2048^2, the time of calculation was doubled in order to be convinced of the establishment of statistical equilibrium. We designate the space averaging as follows: $8192^2 \to 128^2$, where 8192^2 is the initial grid and 128^2 is the rough grid, each value of which is obtained by averaging over the area 64×64.

In Fig. 1, we show the general view of the solutions in viscid and inviscid problems at the highest resolu-

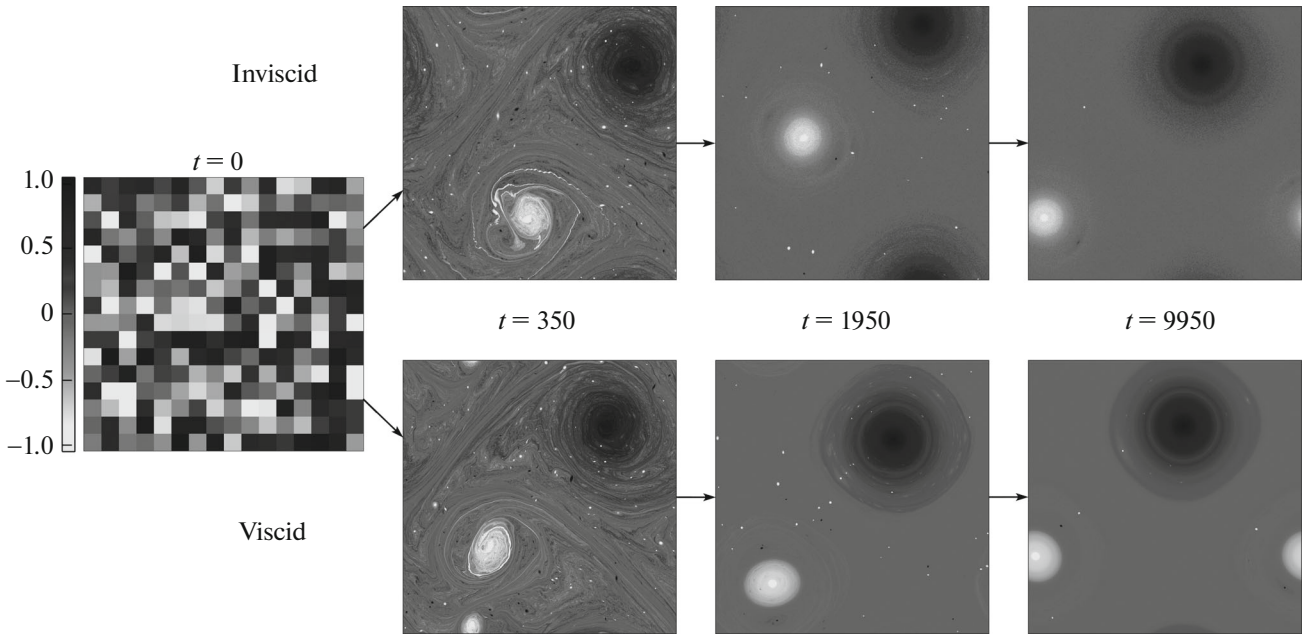

Fig. 1. Vorticity field at various moments of time. The average inviscid problem $8192^2 \to 512^2$ above and viscous 8192^2 below. The values exceeding the limits of the color band are tinted by extreme colors of this band.

tion of 8192^2. For the inviscid problem, we preliminarily averaged the vorticity field, thus separating the large-scale coherent structures from the fine-scale fluctuations. In the solutions, coherent structures are observed in two characteristic scales: large vortices, which have the scale of the region, and fine vortices, which are located in the wavenumber range from 50 to 70. By the moment of time $t \approx 2000$, the formation of two large vortices is accomplished. Further, the variability is associated with the destruction of fine vortices. From the moment $t = 1950$ to $t = 9950$, the number of fine vortices decreases from 50 to 6 in the viscid problem and from 27 to 1 in the inviscid problem. In the latter case, the fine-scale fluctuations promote the destruction. Fine vortices were found only under the highest resolution of 8192^2.

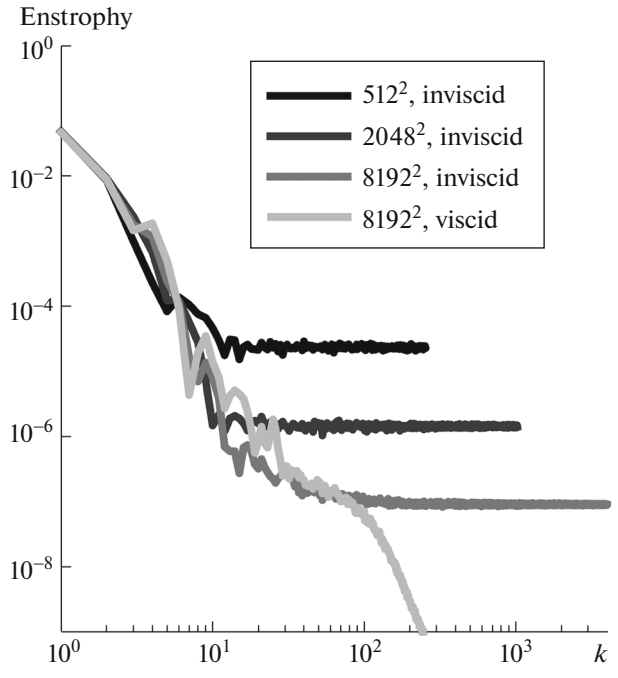

Fig. 2. Enstrophy distribution over the wave-number spectrum normalized to one mode $Z(k)/(2\pi k)$, where $Z = \int Z(k)dk$, $t = 10\,000$, k is the wave number.

In Fig. 2, we show the enstrophy spectrum per Fourier mode for various experiments. In all inviscid problems in fine scales, the equidistribution of enstrophy over the Fourier modes is observed, which agrees well with the spectral theory [9]. In this region, the fine-scale fluctuations are concentrated. With increasing resolution, the left boundary of this region is displaced to the right releasing ever more large scales from fluctuations. The enstrophy spectrum in large scales is practically independent of the resolution or of the presence of viscosity. Contrary to the mean field theory, there is no full condensation of energy to the largest harmonic in the inviscid problem. Moreover, there is not even the tendency to condensation upon increasing the resolution 16 times. The high-order casimirs in the inviscid problem are not conserved, and their average value in time is practically independent of the resolution (figure is not presented).

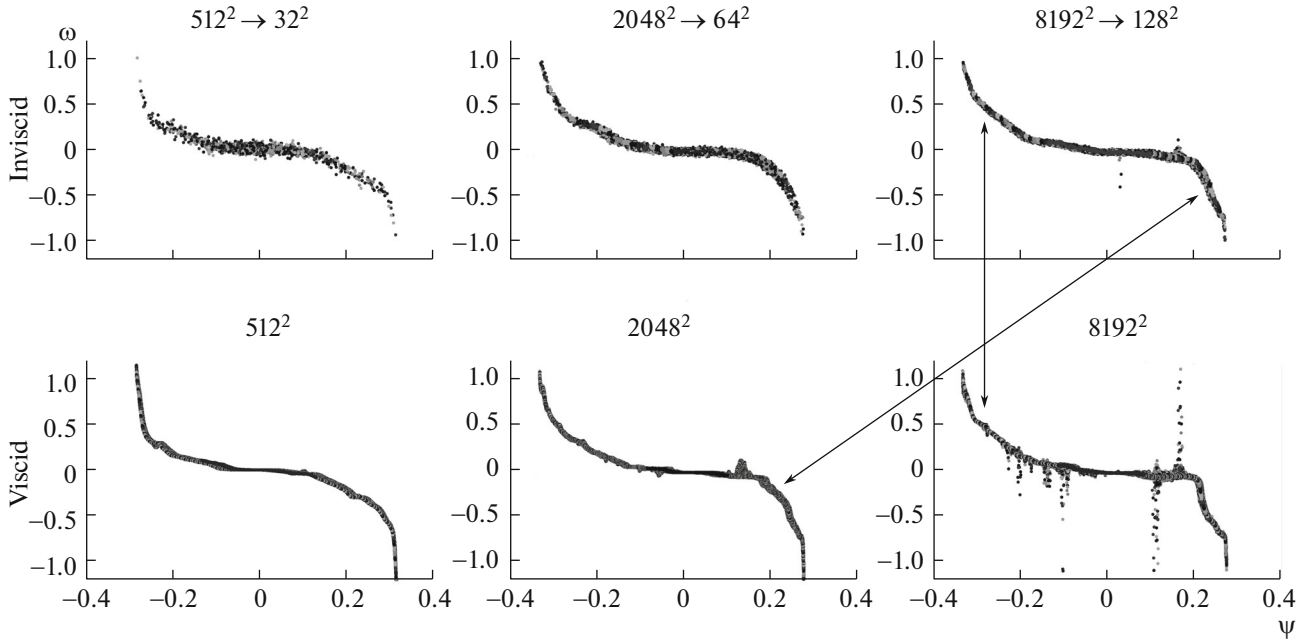

Fig. 3. Scatter plot $\omega - \psi$ at various resolutions: above, space-averaged inviscid problems; below, viscous problems, $t = 10000$.

We study the shape of the coherent structures considering the scatter plot $\omega - \psi$, which is shown in Fig. 3. The inviscid problem is preliminarily averaged over space. The averaging $8192^2 \to 128^2$ is chosen from the reasons of filtration of all wave numbers above 64, where the fine-scale fluctuations are located (see Fig. 2). At low resolutions, the diagram has a symmetric form, and the symmetry is violated with increasing the resolution: sharp bends (corresponding to the step shape of large vortices) and spikes (corresponding to fine vortices) arise; similar branches of the diagram for viscid and inviscid problems are marked in the figure with arrows. With increasing the resolution in the inviscid problem, the spread in points with respect to the functional dependence $\omega = F(\psi)$ gradually decreases, and it evidences that the coherent structures become ever more steady and approach the equilibrium states of an ideal fluid with a certain set of values of invariants [3]. It should be noted that this functional dependence differs from the theoretical (linear) because of the incomplete condensation of energy, which was already reported above.

Diameter of the large-vortex orbit with positive vorticity

Resolution	Orbit diameter	
	viscid problem	inviscid problem
512^2	5.67	chaos
2048^2	1.30	2.5
8192^2	0.79	1.55

We consider the process of obtaining coherent structures with the help of time averaging (Cesaro convergence). The large vortices drift accomplishing translatory (the vector connecting two vortices remains constant) periodic motion along a circular orbit. In the inviscid problems at low resolutions, this motion passes into chaotic motion because of the action of fluctuations on large scales. In the table, the diameter of the circular drift orbit is listed. The orbit diameter monotonically decreases with increasing resolution; however, this result can be nonuniversal because, in certain viscous experiments at low resolutions, we found the reverse tendency. In the inviscid experiment at the highest resolution of 8192^2, the orbit diameter is of the same order of magnitude with the vortex-core size. For this reason, time averaging results in smoothing the large scales. The resulting scatter plot $\langle\omega\rangle - \langle\psi\rangle$ (we do not present the corresponding figure) differs strongly from the classical $\bar{\omega} - \bar{\psi}$: there is no visual similarity, the range of vorticity values is small, and, most importantly, the dependence $\langle\omega\rangle = G(\langle\psi\rangle)$ is nonmonotonic, which prohibits the existence of such coherent structures in an ideal fluid [3].

In summary, the quasi-equilibrium states of the equations of a viscous fluid and the finite-dimensional approximations of the equations of an ideal fluid comprise fine vortices, while large vortices have a similar shape and have a step structure. Contrary to the mean field theory, there is no full condensation of energy in the finite-dimensional approximations, and the enstrophy spectrum coincides with the spectrum of

the viscous fluid on large scales. The coincidence of the large-scale dynamics leads us to the important conclusion that, for the reproduction of the statistical properties of the viscous fluid, it is unnecessary to pay attention to the preservation of high-order casimirs as was done in the mean field theory. It was shown that the degree of unsteadiness of the large scales (i.e., the drift orbit) can decrease with increasing resolution; however, for investigating the possible disappearance of unsteadiness, it is necessarily a considerably higher resolution. The application of the Cesaro-convergence theory did not solve the problem of unsteadiness of the final states because time averaging smooths physically important large-scale structures.

ACKNOWLEDGMENTS

The authors thank A.V. Glazunov and E.V. Mortikov for useful remarks, and also the management of the SRCC of Moscow State University, for the opportunity to carry out numerical calculations on the Lomonosov-1 supercomputer.

This work was fulfilled in the Institute of Numerical Mathematics, Russian Academy of Sciences, and supported by the Russian Science Foundation, project no. 14-27-00126 (comparison of viscid and inviscid problems), and a grant of the President of the Russian Federation, project no. NSh-9836.2016.5.

REFERENCES

1. V. Kozlov, *Gibbs Ensembles and Nonequilibrium Statistical Mechanics* (NITs RKhD, IKI, Izhevsk, 2008) [in Russian].
2. A. Arakawa, J. Comput. Phys. **1** (1), 119 (1966).
3. F. Bouchet, Physica D: Nonlin. Phenomena **237** (14), 1976 2008.
4. F. Bouchet and M. Corvellec, J. Statist. Mech.: Theory and Exp. **08** (P08021) (2010).
5. C. Cichowlas, P. Bonaпti, F. Debbasch, and M. Brachet, Phys. Rev. Lett. **95** (26), 264502 (2005).
6. D. Dritschel, W. Qi, and J. Marston, J. Fluid Mech. **783**, 1 (2015).
7. U. Frisch, S. Kurien, R. Pandit, W. Pauls, S. Ray, A. Wirth, and J. Zhu, Phys. Rev. Lett. **101** (14), 144501 (2008).
8. R. Kraichnan, Phys. Fluids **10** (7), 1417 (1967).
9. R. Kraichnan, J. Fluid Mech. **67** (01), 155 (1975).
10. W. Matthaeus, W. Stribling, D. Martinez, S. Oughton, and D. Montgomery, Phys. Rev. Lett. **66** (21), 2731 (1991).
11. W. Qi and J. Marston, J. Statist. Mech.: Theory and Exp. **7** (P07020) (2014).
12. R. Robert and J. Sommeria, J. Fluid Mech. **229**, 291 (1991).
13. A. Venaille, T. Dauxois, and S. Ruffo, Phys. Rev. E **91** (1), 011001 (2015).

Translated by V. Bukhanov